JOURNAL OF GUIDANCE, CONTROL, AND DYNAMICS
Vol. 20, No. 3, May–June 1997

Piezoelectric Stack Actuators and Control System Design: Strategies and Pitfalls

John A. Main* and Ephrahim Garcia†
Vanderbilt University, Nashville, Tennessee 37235

An evaluation is presented of two control strategies for piezoelectric stack actuators: voltage feedback control and charge feedback control. The study consists of two principal parts: an experimental determination of the nonlinearities inherent in piezoelectric actuators using different control strategies and an analysis of how those nonlinearities would affect the stability and performance of feedback control systems that utilize piezoelectric actuators. The voltage control response of the piezoelectric actuator tested was demonstrably more nonlinear than the same actuator with charge feedback circuitry. Nyquist design analysis reveals that these nonlinearities translate into lower stability margins and potential system performance for voltage control of piezoelectric actuators as compared to charge control. The improved system stability that can be achieved with charge control as compared to voltage control is demonstrated to be significant in multi-degree-of-freedom systems but almost negligible when the system dynamics are essentially single degree of freedom.

Nomenclature

A	= stack cross-sectional area, m^2
C	= series capacitance, F
c^D	= modulus at constant electric displacement, Pa
c^E	= modulus at constant electric field, Pa
D	= electric displacement, coulomb/m^2
E	= total electric field, V/m
e, d, h, g	= piezoelectric constants
F	= force applied to tip mass, N
G	= voltage amplifier gain
K_c	= controller subsystem
K_f	= displacement feedback subsystem
K_g	= gain margin, dB
K_m	= stack/mechanism subsystem
m	= target mass, kg
N	= system describing model discrepancies
n	= number of stack layers
Q_t	= total charge applied to stack, coulombs
S	= strain
T	= stress, Pa
t	= stack layer thickness, m
V	= voltage applied to stack, V
V_{in}	= amplifier input voltage, V
x	= displacement, m
χ	= phase margin, deg

Introduction

BECAUSE of their size and ability to apply significant forces over a small displacement range, piezoelectric actuators have entered the mainstream of mechanical system design in applications where their unique properties provide a design solution. They are commonplace as positioners in scanning-tunneling microscopes, vibration dampers, and focusing elements in adaptive optical systems. This increasing use of piezoelectric actuators indicates that they have reached a critical point in the evolution of a mechanical component. Piezoelectric actuators are now reliable and readily available, making them a practical design option for application of controlled forces and motions in mini- and microdevices.

Received Jan. 8, 1996; revision received Jan. 24, 1997; accepted for publication Jan. 25, 1997.

*Research Assistant Professor, Smart Structures Laboratory, Department of Mechanical Engineering; currently Assistant Professor, Department of Mechanical Engineering, University of Kentucky, Lexington, KY 40506-0108. Member AIAA.

†Associate Professor, Smart Structures Laboratory, Department of Mechanical Engineering. Member AIAA.

A key issue in incorporation of components in the design mainstream is the ability of the system engineer to predict performance at both the component and system levels so that intelligent and informed design decisions can be made. Accurate system models are critical to project success in an environment where the length of product design cycles is decreasing and product testing takes place in virtual environments. In modern engineering accurate component models are a necessity, not a luxury; therefore, a critical look needs to be taken at the models of piezoelectric actuators. The goal of this investigation is to specifically look at the accuracy of models of piezoelectric stack actuators (stacks).

There are many different models for piezoelectric actuators in the literature.[1–4] Fundamentally, though, models fall into two categories: those that are based on a voltage-proportional constitutive relationship and those that are based on a charge-proportional constitutive relationship.[5] The purpose of this paper is to investigate the two available constitutive-based models and examine how stack behavior deviates from model predictions in each case. The overall purpose is not to develop a new model or improve an old one, but to examine how the deviations of the behavior of the actuator from the model can impact design decisions in systems that include piezoelectric stacks.

Method

This investigation was undertaken to answer the questions: How good are the models for piezoelectric stacks, and how might deviations from those models affect design decisions in systems that include stack actuators? It is evident that there are two distinct tasks involved in answering these questions. The first is largely an experimental task, determination of the differences between a physical system (the stack) and its analytical model. The second is a theoretical exercise, predicting how the discrepancies will impact the overall design of some other system that incorporates piezoelectric stacks.

The physical system examined in this case is shown in Fig. 1. It is a simple stack actuator with an aluminum tip mass securely mounted to a massive optical table. The purpose of the tip mass is to provide a conductive target for a capacitance displacement sensor. This particular system was chosen so that the characteristics of the stack actuator would predominate and so that any deviations from the analytical models that might be noted during system testing would be due to the stack only. Because the only other component in the physical system is a mass, and the dynamic characteristics of mass are well known, any deviations of the physical system from the model predictions can be safely assumed to be characteristics of the stack.

In a previous investigation, two strategies for the control of piezoelectric stack actuators were presented.[5] These two strategies are

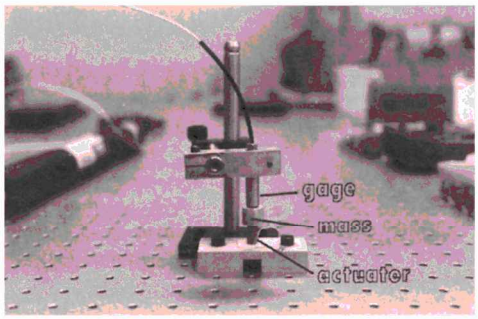

Fig. 1 Photograph of the system test setup showing the piezoelectric stack actuator, driven mass, and capacitance displacement gauge.

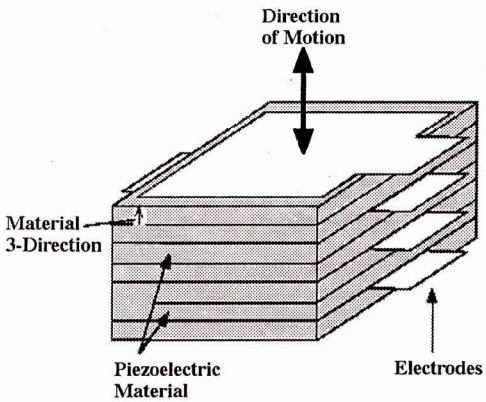

Fig. 2 Sketch of a piezoelectric stack actuator.

derived through different approximations of the piezoelectric constitutive equations, but fundamentally the difference is that one relies on control of the voltage applied to a stack and the other on the charge applied to a stack. The relationship for controlling the load/deflection characteristics of a piezoelectric stack with applied voltage can be derived from one of the standard forms of the piezoelectric constitutive relationships,[6]

$$T_p = c^E_{pq} S_q - e_{kp} E_k \tag{1}$$

where T is the stress applied to the piezoelectric stack, c^E the material modulus at constant electric field E, S the strain in the piezoelectric material, and e the piezoelectric constant. The constant e is not the piezoelectric constant that is typically supplied, and so the substitution

$$e_{kp} = d_{kq} c^E_{qp} \tag{2}$$

is used to put the equation in terms of the more familiar piezoelectric constant d. In addition, if the actuator has a geometry similar to Fig. 2, where all stresses and fields are limited to the 3 direction, the constitutive relationship can be accurately approximated by

$$T_3 = c^E_{33} S_3 - d_{33} c^E_{33} E_3 \tag{3}$$

where contributions from directions other than the 3 direction are neglected.

For a particular stack actuator the strain in the 3 direction can be written as

$$S_3 = x/nt \tag{4}$$

where x is the actuator tip deflection.

Controlling the piezoelectric actuator with voltage is based on the assumption that the field applied to a piezoelectric material is equivalent to the total field present in the material. This is not strictly true,[5] but it is a useful approximation because it relates the field term E to an easily controllable quantity, namely, a voltage V applied to two electrodes on either side of a wafer of piezoelectric material,

$$E_3 \approx V/t \tag{5}$$

Making the substitution and noting that $T_3 = F/A$, where F is the actuator applied force, a control relationship for piezoelectric stacks is found that describes the relationship between the applied voltage and the output force and deflection,

$$F = \frac{Ac^E_{33}}{nt} x - \frac{Ad_{33} c^E_{33}}{t} V \tag{6}$$

The practical implementation of this control scheme can be accomplished with a simple inverting amplifier. If the output of the system is taken to be the displacement of the tip mass, the equation of motion can be derived by examining the free-body diagram of the system in Fig. 3:

$$m\ddot{x} = -\frac{Ac^E_{33}}{nt} x - \frac{Ad_{33} c^E_{33} G}{t} V_{\text{in}} \tag{7}$$

where $-G$ is the gain of the inverting voltage amplifier and the coordinate x is actuator extension.

Taking V_{in} as the system input and x as the system output results in the block diagram shown in Fig. 4a that describes the dynamic behavior of this simple system. The stack is assumed to be massless in this simple one-degree-of-freedom model. The transfer function equivalent to this diagram is

$$\frac{x}{V_{\text{in}}} = \frac{-\left(Ad_{33} c^E_{33} G/t\right)}{ms^2 + \left(Ac^E_{33}/nt\right)} \tag{8}$$

A similar line of reasoning can be used to develop a stack control relationship and system transfer function that relies fundamentally on charge applied to the actuator. The piezoelectric constitutive relationship in Eq. (1) can be written in terms of different state variables as[6]

$$T_i = c^D_{il} S_l - h_{ij} D_j \tag{9}$$

As in the voltage control case, h is a value that is not generally supplied by manufacturers, and so the substitution

$$h_{ip} = g_{iq} c^D_{qp} \tag{10}$$

is used to switch to the more common piezoelectric constant g.

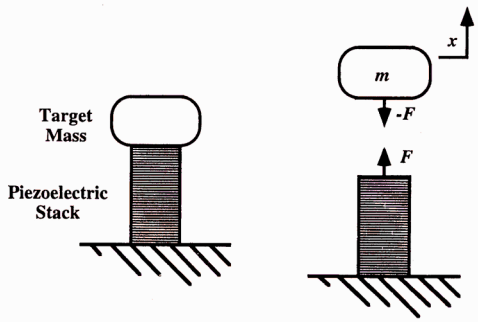

Fig. 3 Free body diagram of the stack-mass positioning system.

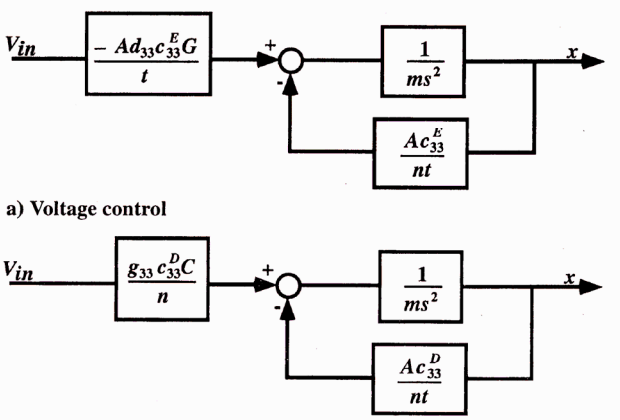

Fig. 4 Block diagram of the stack-mass positioning system.

The constitutive relationship can be approximated by

$$T_3 = c_{33}^D S_3 - g_{33} c_{33}^D D_3 \tag{11}$$

where again only the 3-direction contributions are assumed to be significant.

The electric displacement in the 3 direction (D_3) can be expressed in terms of the charge applied to the stack by applying Gauss' law for dielectrics. This results in the relationship

$$D_3 = Q_t / nA \tag{12}$$

where Q_t is the total amount of the charge applied to the stack.[5] Applying this substitution, as well as those for stress and strain, results in the following control relationship for the charge-activated piezoelectric actuator:

$$F = \frac{Ac_{33}^D}{nt} x - \frac{g_{33} c_{33}^D}{n} Q_t \tag{13}$$

Applying a known amount of charge to a stack requires a different amplifier configuration than in the voltage control case. Charge control of piezoelectric actuators has been demonstrated by a number of investigators,[7–9] and a relatively simple circuit that will apply a known amount of charge is shown in Fig. 5 (Ref. 10). Circuit analysis shows that the charge applied to the piezoactuator is

$$Q_t = C V_{\text{in}} \tag{14}$$

The value of the series capacitance C is the effective charge-feedback amplifier gain in coulombs per volt. Using these results, the equation of motion for the tip mass in the charge control case can be written

$$m\ddot{x} = -\frac{Ac_{33}^D}{nt} x + \frac{g_{33} c_{33}^D C}{n} V_{\text{in}} \tag{15}$$

and the system block diagram drawn as shown in Fig. 4b. The system transfer function that is equivalent to this diagram is

$$\frac{x}{V_{\text{in}}} = \frac{g_{33} c_{33}^D C / n}{ms^2 + \left(Ac_{33}^D / nt\right)} \tag{16}$$

Equations (8) and (16) represent single-degree-of-freedom dynamic models of the stack-mass system under voltage and charge control, respectively. The stated purpose of this investigation is to quantify the accuracy of these models and determine how any inaccuracies will affect system design decisions. This requires some sort of methodology to catalog the differences between the models and actual system behavior.

The describing function method of nonlinear system analysis is used here to reduce experimental data and provide a framework for a stability analysis. Numerous other methods for modeling the real response of piezoelectric materials to electrical inputs hysteresis are present in the literature. Often they focus on modeling actuator hysteresis (for example, see Ref. 11). The describing function approach

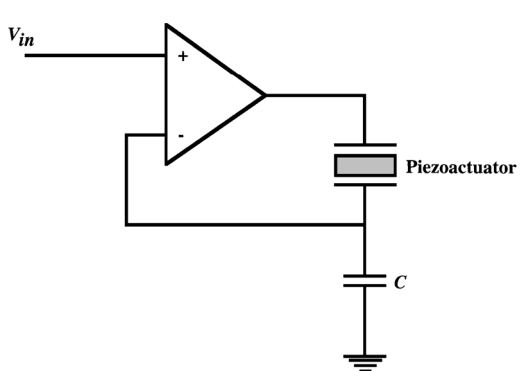

Fig. 5 Amplifier configuration to control charge applied to a piezoelectric actuator.

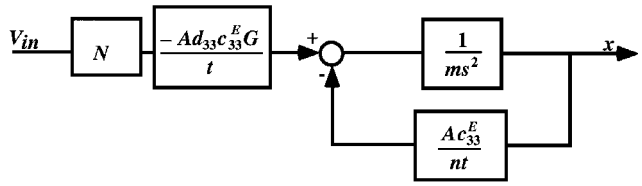

Voltage control

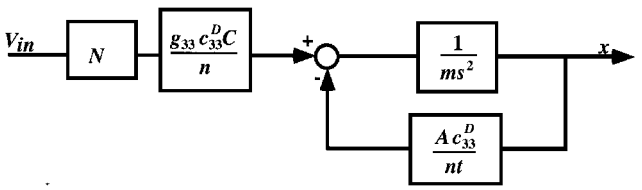

Charge control

Fig. 6 Block diagrams for the stack-mass positioning system including the arbitrary block *N*.

was chosen for this investigation because of the ease in which it is incorporated into control system analyses.

The basis of the describing function method[12] is the addition of a nonlinear block, labeled N, to the system block diagrams (see Fig. 6). In typical describing function stability analyses this block is used to add a known nonlinear effect, such as gear backlash or static friction, to an otherwise linear system. Here N will be used as an arbitrary complex gain that describes the differences between the system model predictions and the true system behavior. Obviously, if the system and model agree completely, N will always equal 1. Similarly, if the difference between the model and the physical system is some unmodeled linear phenomenon, such as viscous damping or a lag in the actuator response, N will have a constant complex value or may vary only with frequency.

Values for N are calculated by equating experimental test results for x/V_{in} to the transfer functions from the block diagrams in Fig. 6. Solving for N yields

$$N(f, X) = \left(\frac{x}{V_{\text{in}}}\right)_{\text{experimental}} \frac{ms^2 + \left(Ac_{33}^E / nt\right)}{-\left(Ad_{33}c_{33}^E G / t\right)} \tag{17}$$

in the voltage control case and

$$N(f, X) = \left(\frac{x}{V_{\text{in}}}\right)_{\text{experimental}} \frac{ms^2 + \left(Ac_{33}^D / nt\right)}{g_{33}c_{33}^D C / n} \tag{18}$$

in the charge control case, where N is assumed to be a function of both frequency f and amplitude X. Calculating the differences between the models and the experimental data in this fashion allows the results to be analyzed in a manner similar to a Nyquist system design exercise, revealing system stability and performance limits. This will be shown in detail in the following sections.

Experimental Procedures

The behavior of the amplifier-stack-mass system was evaluated in both the voltage and charge control configurations by applying a sinusoidal input signal to each of the amplifier embodiments (voltage feedback and charge feedback) and recording the cyclic displacement output of the mass with a capacitance displacement gauge. System tests were performed at frequencies of 1, 100, 200, 300, 400, 500, and 600 Hz and at mass displacement amplitudes of 1, 2, 3, 4, 5, and 6 μm, resulting in a total of 42 tests with each amplifier configuration. Raw time histories of the system input and output were digitized and recorded under each set of test conditions.

The frequency range was selected to keep the excitation signal in the quasistatic regime, that is, well below the first natural frequency of the stack-mass system. The amplifiers were also tested and demonstrated no dynamics over the test condition range. Finite element analysis indicated that the lowest natural frequency of the stack-mass system was greater than 10 kHz. This was experimentally confirmed by applying broadband voltage noise to the

stack-mass system and recording the displacement/input voltage transfer function shown in Fig. 7.

The amplitude range was limited by the maximum amount of voltage (or charge) that could be applied to the stack without permanently depoling the piezoceramic. Because piezoceramics can generally withstand greater positive voltages and charges than negative ones, a displacement offset of $+3.75\ \mu$m was applied to the stack in all of the tests by adding an appropriate dc offset to the input signal to put the stack in the middle of the allowable operating range. The actuator properties are listed in Table 1. An inverting amplifier with a gain of 10 was used in the voltage-feedback tests. In the charge-feedback amplifier tests, a 10-μF series capacitor was used, which resulted in an amplifier gain of 10 μC/V.

The experimental data from each test were acquired and stored in the form of amplifier input-displacement output hysteresis loops. An example of the digitized raw data is shown in Fig. 8. This hysteresis loop also illustrates the large position errors inherent to open-loop operation of piezoelectric actuators. To perform the calculation outlined in Eqs. (17) and (18) for each set of test conditions it was necessary to convert the raw hysteresis loop data into a transfer function representation. The experimental curves were approximated by finding the magnitude and phase of the fundamental harmonic. This was accomplished by directly calculating the magnitude of the transfer function from the peak-to-peak magnitude of the hysteresis loops and basing the phase of the transfer function on the width of the hysteresis loop at the x axis. An example of the resulting curve fit is also shown in Fig. 8. In this fashion, an experimental response curve is approximated by a complex transfer function, allowing the experimental data to be substituted into Eqs. (17) and (18). This process was repeated for every set of test conditions and each amplifier configuration, effectively mapping N as a function of frequency and amplitude over the range of the test conditions.

The calculated complex N values are shown in Figs. 9–12, with the magnitude plots for voltage and charge control in Figs. 9 and 11, respectively, which have identical axes for ease of comparison. In both the charge control and voltage control cases, the value used for the appropriate piezoelectric constant in the model (d_{33} or g_{33}) yielded an N with magnitude near 1 in the quasistatic small-amplitude tests (1-Hz frequency and 1-μm amplitude).

The difference in behavior of the stack-mass positioning system between voltage and charge control is immediately apparent when Figs. 9 and 11 are compared. As discussed earlier, if the model accurately reflects the characteristics of the physical system, the value for N should stay near $1 + 0i$ in the complex plane. This is generally true in the charge control case, where the magnitude of N does show a slight upward trend, but varies approximately only 5% over the range of amplitudes tested. This is in stark contrast to the voltage control case, where the magnitude of N varies fully 45% over the same range of stack displacement amplitudes. The identical result can be seen when comparing the phase of N, plotted as a function of amplitude in Figs. 10 and 12. In the voltage control cases, the phase is larger and more variable than in the charge

Table 1 Geometric and material properties of the piezoelectric stack actuator

Material	PZT-5H
Number of layers n	130
Cross-sectional area A	3.46×10^{-5} m^2
Layer thickness t	120×10^{-6} m
d_{33}	568×10^{-12} m/V
c_{33}^E	6.75×10^{10} Pa
g_{33}	23.3×10^{-3} V-m/N
c_{33}^D	11.1×10^{10} Pa
Tip mass m	8.08 g

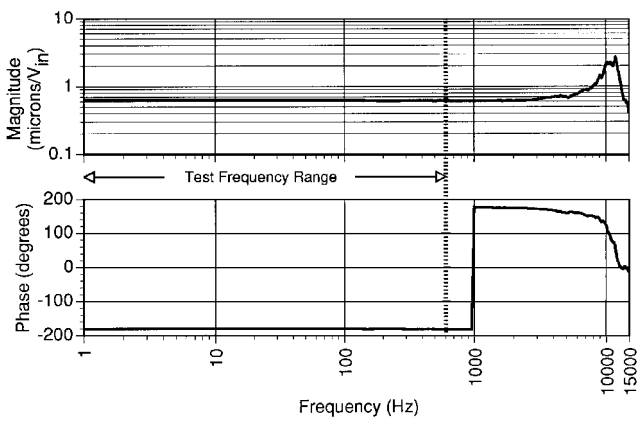

Fig. 7 Transfer function of the stack-mass positioning system under voltage control showing the test frequency range relative to the resonance peak of the system.

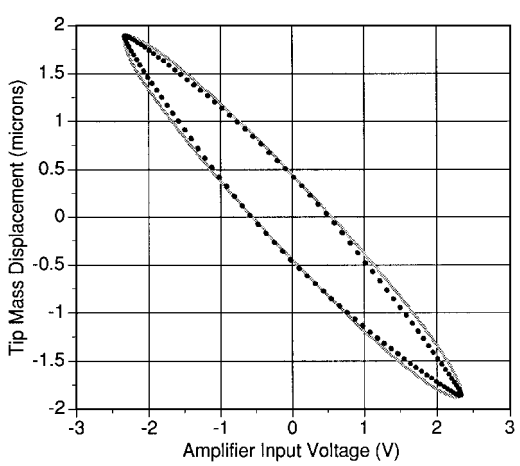

Fig. 8 Example of a digitized input–output hysteresis loop and the fundamental harmonic curve fit.

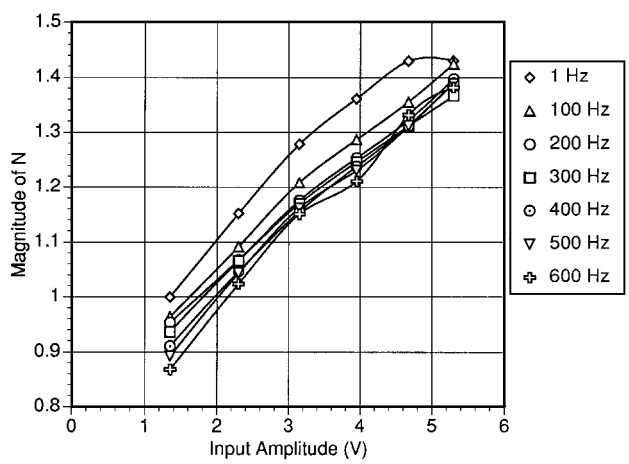

Fig. 9 Plot of the magnitude of N as a function of input voltage amplitude at each test frequency under voltage control.

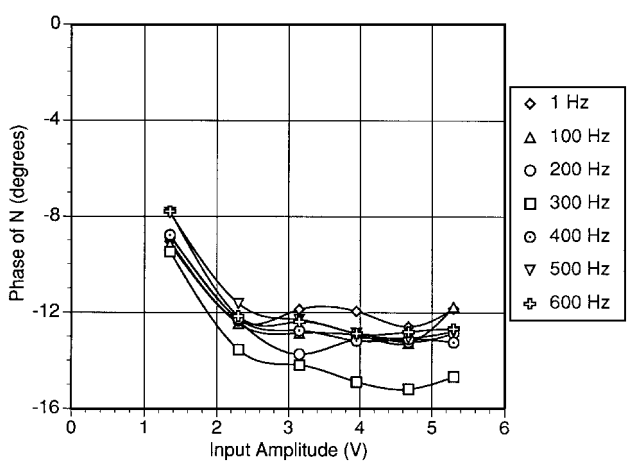

Fig. 10 Plot of the phase of N as a function of input voltage amplitude at each test frequency under voltage control.

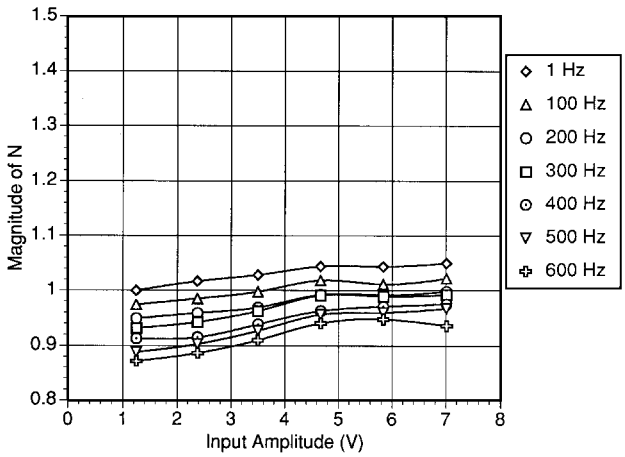

Fig. 11 Plot of the magnitude of N as a function of input voltage amplitude at each test frequency under charge control.

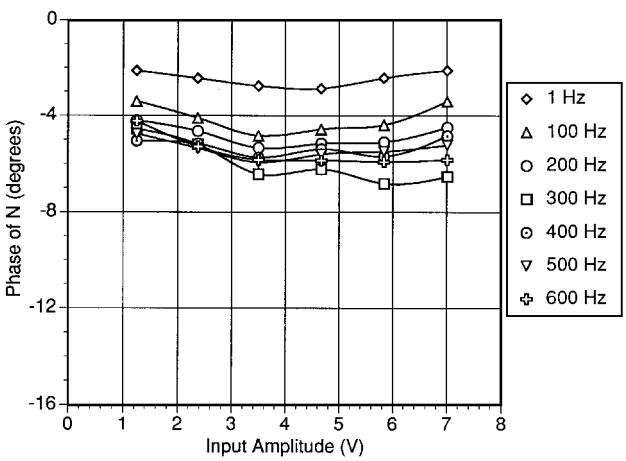

Fig. 12 Plot of the phase of N as a function of input voltage amplitude at each test frequency under charge control.

control cases. Note that the voltage control discrepancies are not variations in piezoelectric constants but exist because the applied electric field is not equal to the total electric field in the piezoelectric material.[5] Differences between model predictions and true system behavior are often attributed to an amplitude dependence in either the piezoelectric constants or the piezoactuator capacitance (for an illustration of both of these effects, see Ref. 9). However, variable piezoelectric constants and/or capacitance can only account for amplitude-dependent changes in the magnitude of the system transfer functions, not the phase variation. The describing function method is used here because it easily accommodates the amplitude dependence of both magnitude and phase. Note that determining describing functions in the manner outlined in this paper is equivalent to determining amplitude-dependent piezoelectric constants if those constants are allowed to be complex.

The describing function results dramatically illustrate the errors inherent in the approximation used in Eq. (5), as well as the difficulty in commanding precise displacements in an open-loop voltage controlled piezoelectric actuator system. It is not clear, however, what effect that these system variations, which are clearly unmodeled nonlinear effects as demonstrated by their amplitude dependence, will have on a closed-loop control system. In the following section, the results of the experimental investigation will be used to predict how these unmodeled nonlinearities will affect the stability and performance of feedback control systems that include a piezoelectric stack actuator.

Feedback-Control Considerations

One common application of piezoelectric stack actuators is in microposition control. A typical system diagram for position feedback control using stacks is shown in Fig. 13, where K_c represents the controller transfer function, K_m the combined transfer function of the stack and the mechanism it is driving, and K_f the transfer function of the position feedback component. The transfer function equivalent of this block diagram is

$$\frac{x}{V_{\text{in}}} = \frac{(K_c + 1)K_m}{1 + K_c K_m K_f} \tag{19}$$

and so the characteristic equation of the system is

$$-1 = K_c K_m K_f \tag{20}$$

In a typical Nyquist stability analysis, the quantity $K_c K_m K_f$ would be plotted on the complex plane and phase and gain margins calculated from the position of the characteristic curve relative to $-1 + 0i$. However, it is clear from the experimental data presented earlier that there can be significant differences between models of stack actuators and the behavior of the physical system, potentially resulting in erroneous stability analyses.

The point is that the true physical system behavior over the range of test conditions was not accurately described by the models of the systems shown in Figs. 5 and 7 in all cases. The true system behavior is best described by the product of the system models [Eqs. (8) and (16)] and the appropriate $N(X, f)$, because by definition N embodies the differences between the model and physical system. By analogy, the true behavior of the stack mechanism in this feedback-control case is not K_m, but is assumed to be NK_m, where the appropriate N is used depending on the control quantity chosen. The characteristic equation can now be written as

$$-1/N = K_c K_m K_f \tag{21}$$

where the quantity $-1/N$ now takes the place of the $-1 + 0i$ point in the Nyquist stability analysis.

The $-1/N$ loci are plotted in the complex plane for four distinct cases in Figs. 14–17. In Figs. 14 and 15, respectively, voltage and charge control describing functions are plotted relative to a curve representing the dynamics ($K_c K_m K_f$) of a single-degree-of-freedom (SDOF) system driven by the piezoelectric actuator. In

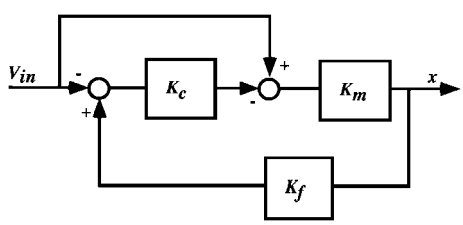

Fig. 13 Block diagram of a typical feedback position control system using piezoelectric actuators.

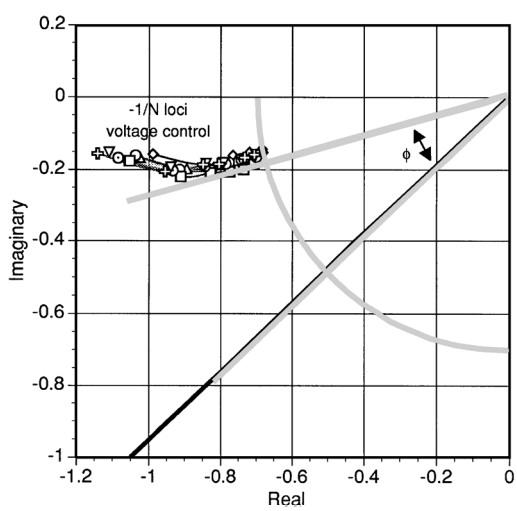

Fig. 14 Calculation of the phase margin for a hypothetical SDOF system with feedback control using voltage controlled piezoelectric stack actuators.

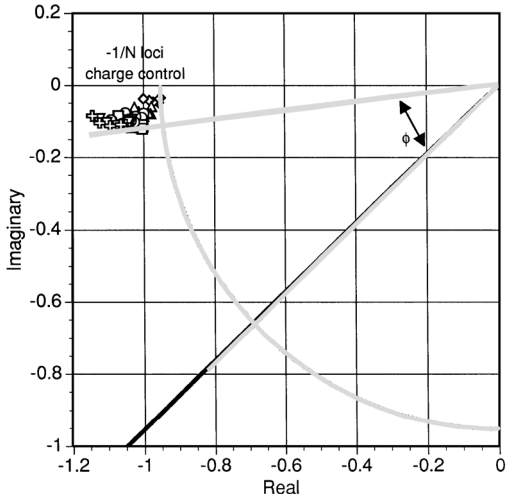

Fig. 15 Calculation of the phase margin for a hypothetical SDOF system with feedback control using charge controlled piezoelectric stack actuators.

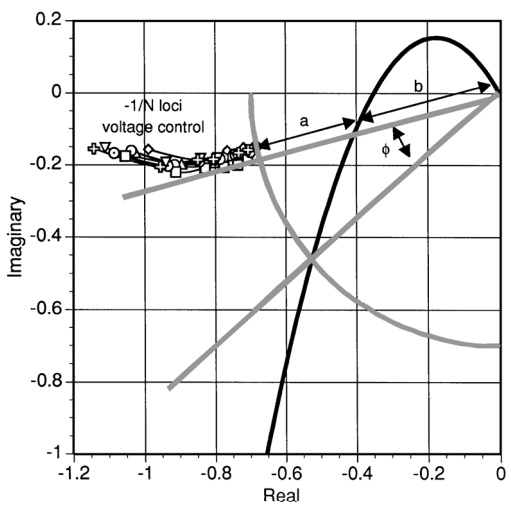

Fig. 16 Calculation of the phase and gain margins for a hypothetical MDOF system with feedback control using voltage controlled piezoelectric stack actuators.

Figs. 16 and 17, the same describing functions are shown with a multiple-degree-of-freedom (MDOF) $K_c K_m K_f$. Because the $-1/N$ loci are serving the purpose that the $-1 + 0i$ point serves in normal Nyquist control system analysis, the relationship between the loci and the characteristic curves can be used to determine gain and phase stability margins in each distinct case.

The calculation of the phase margins for the SDOF case using voltage control and charge control is shown in Figs. 14 and 15. The role of the negative real axis in Nyquist stability axis is played by a radial line that is rotated clockwise until it intersects points from the $-1/N$ loci. The unit circle is replaced by a circle that is expanded about the origin in the complex plane until it also intersects points from the $-1/N$ loci. The phase margin χ is the angle between the negative real axis line and a radial line drawn through the intersection of the characteristic curve and the unit circle.

Performing these geometric constructions yields a phase margin in the case of the SDOF system of 28 deg in the voltage control case and 36 deg in the charge control case. Gain margins in both the charge and voltage control SDOF cases are infinite because the characteristic curve never crosses the negative real axis line. These results indicate that some advantage (an 8-deg improvement in phase margin in this case) can be had by using charge control in SDOF feedback control applications, but the gains are hardly dramatic.

However, Figs. 16 and 17 tell a different story in the case of a piezoelectric actuator driving an MDOF system. The characteristic

Table 2 Results of the stability analyses

	SDOF		MDOF	
	Gain margin	Phase margin, deg	Gain margin, dB	Phase margin, deg
Voltage control	∞	28	4.35	25
Charge control	∞	36	8.11	45

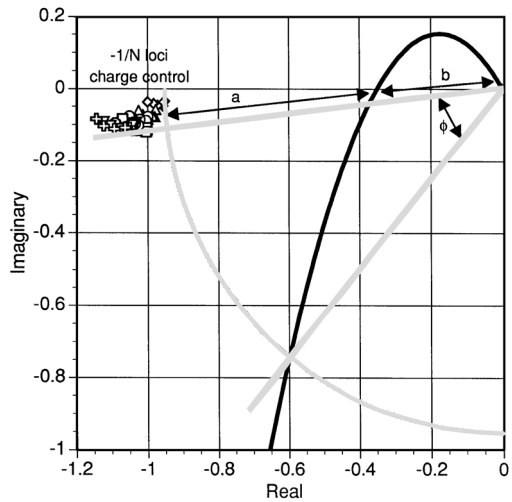

Fig. 17 Calculation of the phase and gain margins for a hypothetical MDOF system with feedback control using charge controlled piezoelectric stack actuators.

curve of an MDOF system will cross the negative real axis some distance from the origin because of the higher-order dynamics present. The system gain curve shown in Figs. 16 and 17 is hypothetical, but it is a reasonable representation of an MDOF characteristic equation. Gain margins are finite in this case and are calculated from the radius of the unit circle and the distance from the origin to the intersection of the characteristic equation and the negative real axis line according to the relationship

$$K_g = (a + b)/b \tag{22}$$

where K_g is the resulting gain margin and a and b are as defined in Figs. 16 and 17.

In the case of the hypothetical MDOF characteristic equation presented here, the gain margin is calculated to be 4.35 dB for voltage control, but significantly higher at 8.11 dB for charge control. Phase margins present the same trend, where the 25-deg stability margin for voltage control is less than the 45-deg margin for charge control. Calculated stability margins are summarized in Table 2 and are significant in two ways. First, in the case of the MDOF system significantly larger gain and phase margins indicate greater system stability and reliability for charge control of piezoelectric actuators than voltage control. Second, larger stability margins mean higher controller gains are possible, potentially increasing system performance and decreasing sensitivity to parameter variation.

The amplitude dependence of the voltage control system has a major impact on this stability analysis. The $-1/N$ loci from the voltage control tests move toward the origin as the amplitude of the input voltage, and thus the stack displacement, increases. It is this behavior that causes the marked difference in the stability comparison between the SDOF and MDOF cases. When using voltage controlled piezoelectric actuators special care should be taken when generalizing the results of SDOF tests to possible applications in MDOF systems. This also means that any given system with voltage controlled piezoelectric actuators, and to a lesser extent charge controlled actuators, could be tested and appear perfectly stable at low amplitudes but if driven at higher amplitudes could exhibit instabilities. Similarly, if phase and gain margins are calculated from

constitutive models, they may be overly optimistic in both voltage and charge control, and the case of voltage control potentially grossly optimistic.

Conclusions

Both voltage control and charge control of piezoelectric stack actuators were investigated over a range of frequencies and amplitudes. Some frequency dependence was observed using both control schemes, likely due to unmodeled damping. Clearly, nonlinear behavior in the form of amplitude dependence was also evident using both control schemes, but it was particularly conspicuous with voltage control. Discrepancies between the response magnitude predicted by the model and experimental results approached 45% for voltage control over the range of stack amplitudes tested. This compares unfavorably with the less than 5% variation in the charge control case.

These system nonlinearities can be masked by closing the loop with feedback control, but there is still a cost because there are lower stability margins in voltage control than charge control because of the higher degree of nonlinearity. These lower stability margins are particularly significant when the piezoelectric actuator is used as part of an MDOF system. The results of this study indicate that the advantages of charge control over voltage control of piezoelectric actuators are small if the feedback-control system in question has an SDOF but the performance differences quickly become significant when MDOF systems are considered.

Acknowledgments

The authors gratefully acknowledge the support of the National Science Foundation (Contract MSS9350269) with Dev Garg of the Dynamic Systems and Controls Program serving as Monitor and NASA (Contract NAG11484) with Garnett Horner serving as Monitor. Portions of this paper were presented at the 10th Virginia Polytechnic Institute and State University Symposium on Structural Dynamics and Control, Blacksburg, Virginia, May 8–10, 1995.

References

[1]Cross, L. E., "Polarization Controlled Ferroelectric High Strain Actuators," *Journal of Intelligent Material Systems and Structures*, Vol. 2, July 1991, pp. 241–260.

[2]Damjanovic, D., and Newnham, R. E., "Electrostrictive and Piezoelectric Materials for Actuator Applications," *Journal of Intelligent Material Systems and Structures*, Vol. 3, April 1992, pp. 190–208.

[3]Jones, L., Garcia, E., and Waites, H., "Self-Sensing Control as Applied to a PZT Stack Actuator Used as a Micropositioner," *Smart Materials and Structures*, Vol. 3, June 1994, pp. 147–156.

[4]Tzou, H. S., "Design of a Piezoelectric Exciter/Actuator for Micro-Displacement Control: Theory and Experiment," *Precision Engineering*, Vol. 13, No. 2, 1991, pp. 104–109.

[5]Main, J., Garcia, E., and Newton, D., "Precision Position Control of Piezoelectric Stack Actuators Using Charge Feedback," *Journal of Guidance, Control, and Dynamics*, Vol. 18, No. 5, 1995, pp. 1068–1073.

[6]Anon., "IEEE Standard on Piezoelectricity," American National Standards Inst./Inst. of Electrical and Electronics Engineers, ANSI/IEEE Std. 176-1987, Inst. of Electrical and Electronics Engineers, New York, 1988.

[7]Kaizuka, H., and Siu, B., "A Simple Way to Reduce Hysteresis and Creep When Using Piezoelectric Actuators," *Japanese Journal of Applied Physics*, Vol. 27, No. 5, 1988, pp. L773–L776.

[8]Anderson, E., Moore, D., Fanson, J., and Ealey, M., "Development of an Active Member Using Piezoelectric and Electrostrictive Actuation for Control of Precision Structures," *Proceedings of the AIAA 31st Structures, Structural Dynamics, and Materials Conference* (Long Beach, CA), AIAA, Washington, DC, 1990, pp. 2221–2233 (AIAA Paper 90-1085).

[9]Newcomb, C., and Flynn, I., Improving the Linearity of Piezoelectric Ceramic Actuators," *Electronics Letters*, Vol. 18, No. 11, 1982, pp. 442, 443.

[10]Comstock, R. H., "Charge Control of Piezoelectric Actuators to Reduce Hysteresis Effects," U.S. Patent 4,263,527, April 1981.

[11]Dahl, P., and Wilder, R., "Math Model of Hysteresis in Piezo-Electric Actuators for Precision Pointing Systems," *Guidance and Control 1985*, Vol. 57, Advances in the Astronautical Sciences, American Astronautical Society, Univelt, San Diego, CA, 1985, pp. 61–88.

[12]Ogata, K., *Modern Control Engineering*, Prentice–Hall, Englewood Cliffs, NJ, 1970, pp. 538–546.